European Journal of Pharmaceutics and Biopharmaceutics 201 (2024) 114387

Contents lists available at ScienceDirect

European Journal of Pharmaceutics and Biopharmaceutics

journal homepage: www.elsevier.com/locate/ejpb

Light exacerbates local and global effects induced by pH unfolding of Ipilimumab

Elena Rizzotto, Ilenia Inciardi, Benedetta Fongaro, Philipp Trolese, Giorgia Miolo *, Patrizia Polverino de Laureto *

Department of Pharmaceutical and Pharmacological Sciences, Via Marzolo 5, 30131 Padova, Italy

ARTICLE INFO

Keywords:
Monoclonal antibody
Protein drug
pH-induced unfolding
Photostability
Protein aggregation
Protein fragmentation

ABSTRACT

Monoclonal antibodies (mAbs) are an essential class of therapeutic proteins for the treatment of cancer, autoimmune and rare diseases. During their production, storage, and administration processes, these proteins encounter various stressors such as temperature fluctuations, vibrations, and light exposure, able to induce chemico-physical modifications to their structure. Viral inactivation is a key step in downstream processes, and it is achieved by titration of the mAb at low pH, followed by neutralization. The changes of the pH pose a significant risk of unfolding and subsequent aggregation to proteins, thereby affecting their manufacturing.

This study aims to investigate whether a combined exposure to light during the viral inactivation process can further affect the structural integrity of Ipilimumab, a mAb primarily used in the treatment of metastatic melanoma. The biophysical and biochemical characterization of Ipilimumab revealed that pH variation is a considerable risk for its stability with irreversible unfolding at pH 2. The threshold for Ipilimumab denaturation lies between pH 2 and 3 and is correlated with the loss of the protein structural cooperativity, which is the most critical factor determining the protein refolding. Light has demonstrated to exacerbate some local and global effects making pH-induced exposed regions more vulnerable to structural and chemical changes.

Therefore, specific precautions to real-life exposure to ambient light during the sterilization process of mAbs should be considered to avoid loss of the therapeutic activity and to increase the yield of production. Our findings underscore the critical role of pH optimization in preserving the structural integrity and therapeutic efficacy of mAbs. Moreover, a detailed conformational study on the structural modifications of Ipilimumab may improve the chemico-physical knowledge of this effective drug and suggest new production strategies for more stable products under some kind of stress conditions.

1. Introduction

Monoclonal antibodies (mAbs) are an essential class of therapeutic proteins for the treatments of cancer, autoimmune diseases, asthma, viral infections, and other diseases, including infectious, cardiovascular, and central nervous system disorder [1]. These immunoglobulins represent a significant challenge from the pharmaceutical point of view due to their characteristics, such as molecular size, stability, and solubility. Their structure comprises two light (LC) and two heavy (HC) chains brought together by disulfide bridges. The two identical LCs contain a variable (V) and a constant (C) domain. mAb quaternary structure is conventionally divided into three regions, two Fab (antigen-binding fragments) and one Fc (constant fragment). In the Fab domain, the three complementary determining regions (CDRs) are responsible for the specificity of the antibody [2,3]. Due to their structural complexity, the handling of mAbs requires caution. As other biologics, mAbs are exposed to several stresses during their production, storage, and administration. Such stresses can lead to subtle modifications of the protein or cause denaturation with loss of biological activity. Furthermore, the formation of aggregated species in the final formulation can induce reduction of potency and/or immunogenic reactions [4].

Among the environmental stresses able to cause chemical and structural changes to mAbs during the production process, the exposure to acidic conditions during the viral inactivation step and elution from affinity resins appears critical [5–7]. The viral inactivation step involves the titration of the protein samples to low pH under stirring for a specific time and the restoring of neutral pH with a weak base [8]. Low pH conditions may result in protein denaturation and aggregation. Acidic

* Corresponding authors at: Department of Pharmaceutical and Pharmacological Sciences, Via Marzolo 5, 30131 Padova, Italy.
E-mail address: patrizia.polverinodelaureto@unipd.it (P. Polverino de Laureto).

https://doi.org/10.1016/j.ejpb.2024.114387
Received 5 April 2024; Received in revised form 30 May 2024; Accepted 26 June 2024
Available online 27 June 2024

pH can promote formation of non-native protein structures, as partially folded states [9], which exhibit high tendency to aggregate. The stability and dynamics of these acid-induced states are highly dependent on the protein and experimental conditions. Therefore, determination of the pH threshold that separates a definitive protein denaturation and the possibility that the molecule regains its native structure is extremely important, especially for pharmaceutical companies. Indeed, knowing which types of modifications are occurring on the protein after viral inactivation step is to reduce the loss of drug potency during product manufacturing and formulation.

Another environmental factor able to cause protein instability is light exposure. As all proteins, mAbs are photosensitive at the level of tryptophan, tyrosine, phenylalanine, cysteine and cystine, methionine, and histidine. Light exposure can induce both chemical and physical degradation of the polypeptide chains as well as chemical alteration of the ingredients present in formulation buffers. The major pathways of photodegradation for proteins include direct UV light absorption followed by oxidation or photosensitization by internal or external chromophores present in the formulation [10]. Through the absorption of light, mAbs generate singlet or triplet oxygen species and radicals. Moreover, mAbs have been found to catalyze the oxidation of water through the production of singlet oxygen [11]. The reactive oxygen species (ROS) produced under irradiation can contribute to and increase the overall oxidation of the protein. In our previous work, we showed

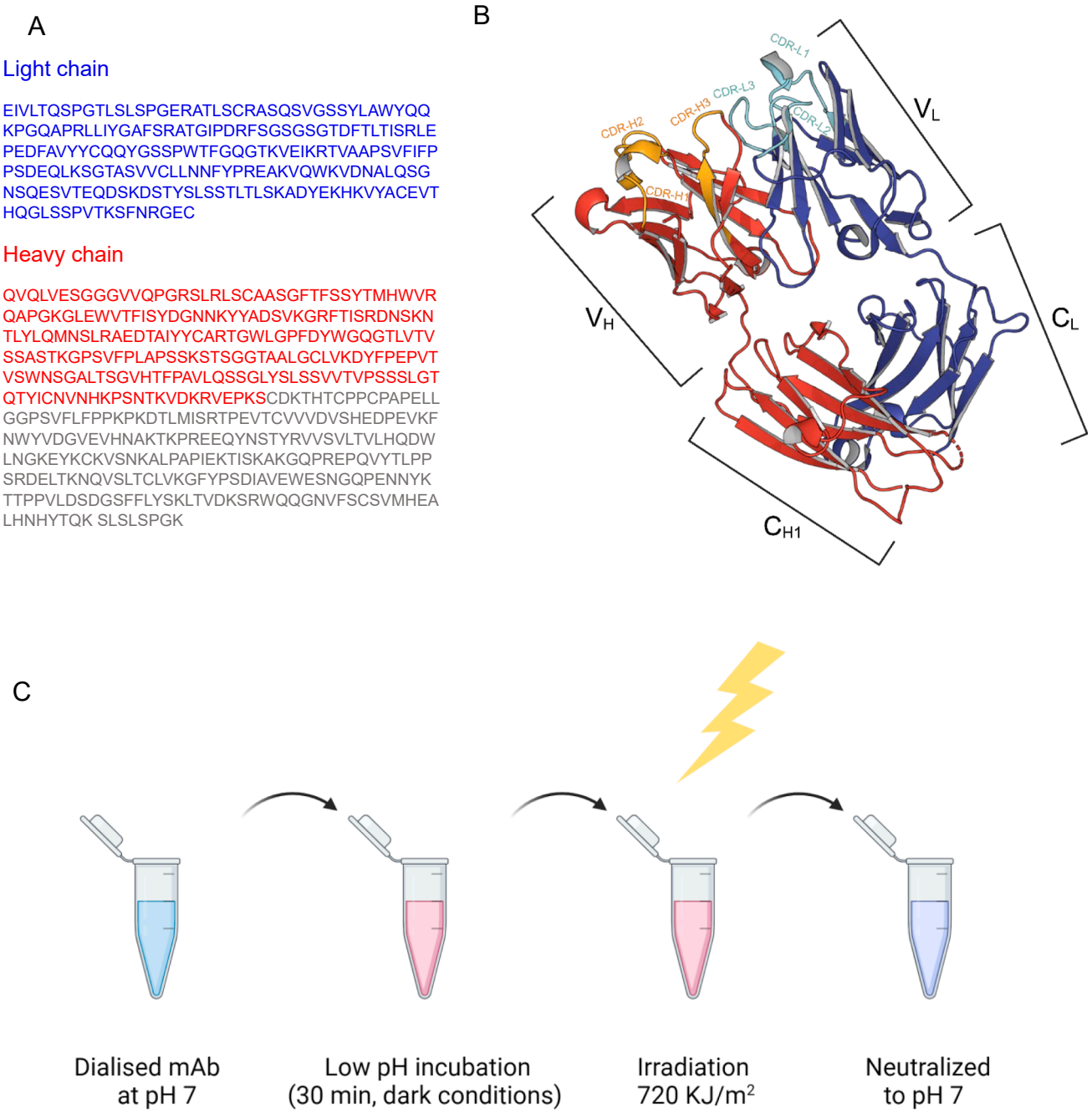

Fig. 1. Amino acid sequence of Ipilimumab (A). Three-dimensional structure of Ipilimumab (PDB code 5TRU) (B). The structure was obtained by using the Pymol software (version 2.5.2). The light chain is highlighted in blue, and the heavy chain is highlighted in red (corresponding to the PDB structure). FC does not appear in the three-dimensional structure and is reported in grey in the sequence. Scheme representing the experimental procedure for mimicking the occurrence of light stress during low pH treatment of the mAb (C). (For interpretation of the references to colour in this figure legend, the reader is referred to the web version of this article.)

how an extreme irradiation condition can exacerbate the formation of aggregated species and the chemical alteration of mAb primary sequence [12]. The combination of low pH (protein unfolding or partially unfolding) and accidental light irradiation may increase the occurrence of the modifications induced by light, which then may trigger protein misfolding and/or aggregation.

The intrinsic stability of the immunoglobulin is another factor to consider during the development of production processes. IgG isotype is divided into four subtypes: IgG1, IgG2, IgG3, and IgG4 [2]. Although the four IgG subclasses are 90 % homologous, they show differences in the hinge region and the N-terminal region of the CH2 domain [13]. The correlation between the different susceptibility to aggregation of IgG subclasses and their conformation stability has not been completely clarified [14,15].

Here, a systemic analytical approach has been applied to understand the structural and conformational changes induced by pH titration and to correlate these to the protein instability propensity after light irradiation. The stability of a specific mAb, Ipilimumab, was tested under low pH conditions and in the presence of light injury. Ipilimumab, a fully humanized IgG1 mAb targeting CTLA-4 on T-cells, is composed of 1326 amino acids with a molecular weight of ~ 145 kDa and a pI of ~ 9 [16–18](Fig. 1A). It contains 24 tryptophan and 60 tyrosine residues and its three-dimensional structure is shown in Fig. 1B. Previously, we have studied Ipilimumab in its formulation (Yervoy®) under the effect of some stressors that could compromise the efficacy of the drug such as light, mechanical stress and temperature fluctuation [12]. Diluted Ipilimumab showed to be sensitive to the minimum dose tested (720 kJ/m^2) representing a situation mimicking a possible risk factor during the production of the mAb that however is an overestimation of light experienced in the protein real-life [19]. After light exposure, Ipilimumab underwent aggregation and chemical modifications of certain residues in the polypeptide chain. However, its formulation, in terms of protein concentration and excipients, guarantees its long shelf life.

In this study, light effect was monitored in accordance with the ICH Q1 (section B) guidelines provided by the European Medicines Agency for confirmatory studies. Spectroscopic techniques have been used to understand the global and local changes induced by titration at different pHs. Moreover, reversibility experiments have been conducted to unravel the recovery of the native conformation lost under low pH and irradiation conditions. Finally, protein aggregation has been assessed by DLS, SEC, and SDS-PAGE. Chemical modification has been analyzed by LC-MS/MS to elucidate the cause of the increased occurrence of high molecular species and to correlate it with protein structural instabilities. To give an insight into conformational and dynamics features of Ipilimumab exposed to low pH and light, a limited proteolysis experiment has been conducted. The rationale of this last procedure is based on the chance to correlate the susceptibility to proteolytic attack to the flexibility of certain regions of the molecule under different experimental conditions. The final aim of this study is to provide knowledge about the behavior of Ipilimumab in relation to changes in pH and to find a pH threshold to assure the molecule refolding. Overall, this study could support pharmaceutical and biotechnological companies to keep precautionary measures to prevent mAb vulnerability to multiple stresses during downstream processing helping to avoid loss or reduction of efficacy. Moreover, a deep conformational study on the structural characteristic of Ipilimumab under different conditions is here presented enriching chemico-physical information on this effective drug.

2. Material and methods

2.1. Material

Commercially available Yervoy®, 5 mg/mL Ipilimumab, (BristolMyers Squibb) was provided by a hospital pharmacy as fresh daily residues after patient treatments. All other chemicals and reagents were of analytical grade and were obtained from Merck (Darmstadt, Germany).

2.2. Methods

Sample preparation. The formulated 5 mg/mL Ipilimumab drug product (Yervoy®) was dialyzed overnight at 4 °C against PBS buffer (20 mM sodium phosphate, 50 mM NaCl at pH 7.4). Dialyzed Ipilimumab aliquots were diluted to 1 mg/mL in PBS at specific pH. The buffer titration to each pH was prepared upon addition drop-by-drop of hydroxyl chloride or sodium hydroxide. The samples were incubated for 30 min at each pH in the dark. The back-titration to pH 7 was conducted using a 2 M solution of 2-amino-2-(hydroxymethyl)propane-1,3-diol (Tris) and checked by a pH meter [8]. The samples were incubated for 30 min before analysis. The temperature for all experiments was set at 25 °C to avoid protein aggregation and degradation [20,21].

Photostability. The tests were performed with a SunTest CPS + instrument (Atlas Technologies GmbH, Linsengericht, Germany). The irradiations were performed in accordance with the ICH Q1B guidelines (https://www.ich.org). Light radiation was generated through a Xenolamp NXE 1500B at a dose of 720 KJ/m^2 (200 W hours/m^2), corresponding to the amount of light the sample would take approximately upon a daily exposure. The irradiance was 360 mW/cm^2 (300–800 nm). Light-protected (dark, wrapped in aluminum foil) samples were used as a control. The temperature was controlled by using a SunCool® device and kept at 22–25 °C. Glass vials with cap were used and set horizontally in the SunTest apparatus.

Spectroscopic techniques. UV–Visible and Second derivative. UV–Visible (UV–Vis) analyses were performed by a V-730 UV–Visible Spectrophotometer (Jasco, Tokyo, Japan) in the 230–350 nm range, using a quartz cuvette with a 1 cm pathlength and a sample concentration of 0.2–1 mg/mL. The spectra were taken at scan speed of 200 nm/min, and a data pitch of 0.1 nm. The second derivative was calculated by the software provided by the manufacturer. The α-value was calculated according to Ragone et al. [22] from Eqs. (1) and (2):

$$r_n = A^{II}(\sim 289nm) - A^{II}(\sim 283nm)/A^{II}(\sim 295nm) - A^{II}(\sim 290nm) \quad (1)$$

$$\alpha - value = (r_n r_\alpha)/(r_u r_\alpha) \quad (2)$$

where the parameter r is obtained as a ratio between the absorbance values of the second derivative spectra at the maxima and minima (eq. (1)); r_n and r_u are the numerical values of this ratio, determined for the native and unfolded protein, respectively; r_a is the numerical value of the ratio determined for a mixture containing the same molar ratio of Tyr and Trp amino acids in ethylene glycol.

Circular dichroism. Circular dichroism (CD) measurements were performed by a Jasco J-810 spectropolarimeter (Tokyo, Japan). Far-UV CD (250–197 nm) spectra were obtained at a sample concentration of 0.2 mg/mL using quartz cells with a 1 mm pathlength, whereas near-UV (350–250 nm) measurements were carried out at a 0.5 mg/mL protein concentration using quartz cells with a 5 mm pathlength. CD signal was expressed as the mean residue ellipticity $[\theta] = \theta_{obs} \cdot MRW/(10 \cdot l \cdot c)$, where θ_{obs} is the observed signal in degrees, MRW is the protein mean residue weight, l is the cuvette pathlength in cm, and c is the protein concentration in g/mL. The sample concentration was determined spectroscopically by using a molar extinction coefficient of 1.6 ml $mg^{-1}cm^{-1}$ (www.expasy.org). Quartz cuvettes were provided from Hellma (Germany, Europe). The samples were centrifuged before analysis and each measurement is obtained by an average of 4 spectra.

Fluorescence. A Jasco FP 6500 fluorimeter equipped with Peltier thermostated single cell holder ETC-273 (Tokyo, Japan) was used for intrinsic fluorescence measurements. Fluorescence measurements were performed using a 1 cm pathlength quartz cuvette at the controlled temperature of 25 °C. Intrinsic fluorescence emission was collected in the 300–500 nm range after excitation at 280 and 295 nm of 0.1 mg/mL concentrated samples. Buffer contribution was removed by its subtraction from protein sample spectra. Measurements were conducted in

triplicates. The instrument calibration is routinely performed according to the procedure provided by the manufacturer (Jasco, Japan).

Limited proteolysis. Limited proteolysis of Ipilimumab was carried out using pepsin [23] and proteinase K [24] at acidic and neutral pH, respectively. The protein concentration was 1 mg/ml. The proteolysis reactions were carried out at 37 °C using an E/S ratio of 1:500 and 1:1000 (by weight). The reactions were quenched at specified times by adding an equal volume of aqueous ammonia (2 %, v/v) in the case of pepsin and by acidification with TFA in water (4 %, v/v) in the case of proteinase K. The proteolytic mixtures were analyzed by SDS-PAGE and RP-HPLC using a C18 column (4.6 mm × 150 mm, The Separation Groups, Hesperia, CA), eluted with a gradient of acetonitrile/0.1 % TFA (v/v) from 5 % to 21 % in four minutes and from 21 % to 46 % in 15 min. The effluent was monitored by recording the absorbance at 226 nm. The sites of proteolytic cleavage were identified by mass spectrometry.

Dynamic Light Scattering. Dynamic Light Scattering (DLS) analysis was conducted by a Zetasizer Ultra (ZSU5700, Malvern instruments, Worcestershire, UK). Sample aliquots were loaded at a concentration of 1 mg/mL. Each measurement was performed in triplicate. Scattering data were analysed with the ZS Xplorer software and expressed by intensity and volume. The appropriate attenuator position was automatically determined by the Zetasizer instrument during the measurement sequence. The mean count rate was between 250 and 350 kcps in all measurements. UV-transparent disposable cuvettes with 0.45 cm pathlength (Sarstedt, Nümbrecht, Germany) were employed. The analysis was conducted in triplicates.

Size exclusion chromatography. Size exclusion chromatography (SEC) was carried out on a High-Performance Liquid Chromatography (HPLC) (Jasco LC-1500, Tokyo, Japan) with a TSKgel® UP-SW3000 column (4.6 × 300 mm, 2 μm; Tosoh Bioscience, Japan) equipped with a TSKgel® UP-SW DC guard column. Samples were eluted with a buffer 0.1 M sodium phosphate / 0.1 M Na_2SO_4, pH 6.7 at a 0.350 mL/min flow rate, detecting at 280 nm. Sample aliquots were loaded at a concentration of 1 mg/mL. The calibration of the column was obtained by loading a mixture of proteins with known molecular weight (Thyroglobulin, Bovine serum albumin, Carbonic anhydrase). Samples were filtered before loading onto the column to remove eventual insoluble aggregates. The analysis was conducted in triplicates.

SDS- and native-PAGE. Electrophoresis in polyacrylamide gel containing SDS (SDS-PAGE) was performed on a 12–15 % T, 2.6 % C, pH 8.8, acrylamide separating gel, and a 5 % T stacking gel according to Laemmli [25]. Prior to loading onto the wells, samples were treated with an SDS-containing sample buffer and boiled at 95 °C for 10 min. The electrophoretic runs were conducted in reducing in the presence of beta-mercaptoethanol or in non-reducing conditions, with a starting current intensity of 9 mA/slab followed by a 12 mA/slab. Native-PAGE was performed on a 10 % T running and 3 % T stacking gel. The running buffer containing 0.4 M β-alanine titrated with glacial acetic acid to pH 4.0 was used. The electrophoretic run was performed with a starting current intensity of 5 mA/slab, and then 25 mA/slab. The electrophoretic runs were performed in a Mini-PROTEAN® Tetra System (BIO-RAD Laboratories Inc., Hercules, California, USA). The staining was done with a Coomassie Blue R-250 solution and the destaining with a water, methanol, and acetic acid solution in a ratio of 50/40/10 (v/v/v). 4 μg of samples were loaded into each well.

Analysis by LC-MS/MS. High resolution mass spectrometry was conducted by the Xevo® G2-XS ESI-Q-TOF mass spectrometer (Waters Corporation, Milford, Massachusetts, USA). For peptide mapping, samples were incubated for 1.30 h at 37 °C with a 50 mM Tris-HCl reducing buffer containing 6 M guanidine hydrochloride at pH 8.5; Tris(2-carboxyethyl) phosphine (TCEP) was added at a 1:10 M ratio on Cys residues to allow the reduction of S-S bridges. Iodoacetamide was used to alkylate (carbamidomethylation) the free cysteine at a 1:10 M ratio on Cys residues for 30 min at 22 °C. The buffer was changed with 100 mM ammonium bicarbonate by Amicon® Ultra 0.5 mL centrifugal filters (Merck Millipore Ltd., Ireland). Tryptic digestion was obtained at a 1:20 trypsin to mAb ratio (w/w). The reaction was left at 37 °C overnight and then stopped by freezing at −20 °C. Proteolytic mixtures were resolved by an UPLC system (Acquity H-Class, Waters Corporation, Milford, Massachusetts, USA) using an AdvanceBio Peptide Map column (2.1 x 150 mm × 2.7 μm; Agilent, Santa Clara, CA, USA). The elution was performed at a flow rate of 0.2 mL/min eluted with the following acetonitrile/0.1 % formic acid − water/0.1 % formic acid gradient: 2–65 %, 36 min, 65–98 %, 2 min. Mass analyses were carried out at 1.5–1.8 kV capillary voltage and 30–40 V cone voltage. Peptide mapping data were processed by BiopharmaLynx, an application manage for MassLynxTM software, using traditional tryptic cleavage rules and setting cysteine carbamidomethylation as a fixed modification and Asn, Gln deamidation, Trp, Met oxidation as variable modifications.

3. Results

3.1. Effect of pH on the structure of Ipilimumab probed by circular dichroism and fluorescence spectroscopy

A spectroscopic characterization of the conformation of Ipilimumab as a function of pH is reported in Fig. 2. The far UV CD spectrum of Ipilimumab at pH 7 resulted from the superposition of the signals deriving mainly from the β-sheet and random coil structures that constitute the most dominant secondary structure elements of mAbs [2]. The far UV CD measurements showed that the protein did not lose completely its secondary β-sheet structure at pH 3, 4 and 9, whereas the spectra at pH 2 and 12 indicated large unfolding (Fig. 2 A1). The tertiary structure was assessed by near UV CD and intrinsic fluorescence. At pH 7, the CD spectrum of Ipilimumab is characterized by two main bands at 273 nm and at 290 nm, as for other mAbs, consistent with the typical profile previously reported [12]. It appeared largely affected at extreme pHs (2 and 12) and less at pH 3 (Fig. 2 A2). The fluorescence emission spectra upon excitation at 280 nm were shown in Fig. 2A3. A slight red shift of the wavelength corresponding to the maximum of the Trp emission was observed when Ipilimumab was exposed at acidic pH, while at pHs above 7 Trp emission underwent a blue shift, indicating that several Trp residues of the protein were differently exposed to solvent. The intensity of fluorescence emission, as a further indicator of localization of Trp residues in the conformational state populated by the protein at a given pH, suggested that the maximum exposure of Trp took place at pH 2, while at pH 3 the molecule appeared more compact and less residues are exposed. In part B of the figure, the ability of the protein to refold upon neutralization of the acidic pH to pH 7 was shown. The refolding spectrum by neutralizing the pH 3 exposed mAb was superimposable to that of the native one, while the recovery of the protein structure resulted non-reversible at pH 2 as deduced by far and near UV CD (Fig. 2, B1 and B2) and intrinsic fluorescence (Fig. 2, B3) spectroscopy.

Overall, our findings provided insights into the pH-dependent conformational dynamics of Ipilimumab, highlighting its structural stability and susceptibility to pH-induced unfolding, which are crucial considerations for therapeutic protein formulation.

3.2. Simultaneous effect of pH changes and light exposure on the structure of Ipilimumab and evaluation of the conformational recovery of the native structure (reversibility)

The conformation of pH 2 and 3 exposed Ipilimumab was analyzed after light irradiation (720 KJ/m^2 light dose). The measurements were done comparing side by side the data obtained in the dark (from samples not exposed to light) (Fig. 3). At pH 7, the fluorescence emission wavelength upon excitation at 280 and 295 nm of irradiated Ipilimumab corresponded to those of the dark samples (Fig. 3A, Table 1), indicating that this light dose alone scarcely affected the structure of the protein. At pH 2, a slight red shift of the wavelength corresponding to the maximum of emission was observed after irradiation (Fig. 3B). No substantial

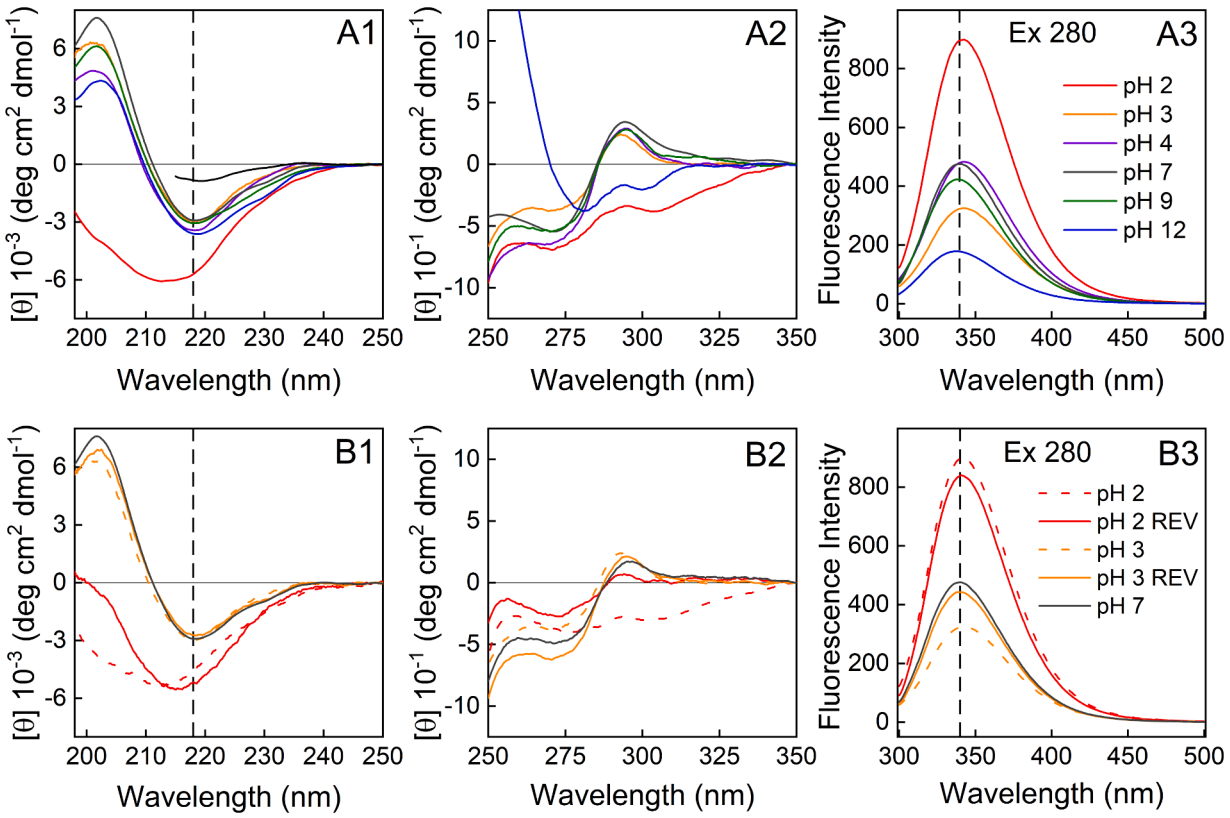

Fig. 2. Structural characterization of Ipilimumab at different pH (A) and after neutralization to pH 7 (B) by far- (A1, B1), near-UV (A2, B2) CD and fluorescence (A3, B3) spectroscopy. Fluorescence spectra are obtained after excitation at 280 nm. Vertical black dashed lines indicate the wavelength corresponding to the β-sheet signal in A1 and B1, and the fluorescence maximum wavelength of emission at pH 7 (A3, B3). The refolding curves from pH 2 and 3 to pH 7 obtained by titrating the solutions are indicated as REV. In A1 the far UV CD spectrum of Ipilimumab in 8 M urea (black line) is reported as a control.

differences were detected for the mAb exposed to pH 3, before and after irradiation (Fig. 3C). The effect of the neutralization of pH after irradiation was analyzed (Fig. 3, B2 and C2). A conformational reversibility was observed only for the mAb incubated at pH 3, irradiated and then titrated to neutrality. Indeed, the wavelength corresponding to the maximum of emission was comparable with that observed at pH 7. For samples incubated at pH 2, irradiated and then titrated to pH 7, the wavelength maximum corresponded to that determined at pH 2, confirming that the denaturation process is irreversible at this pH condition.

To give an insight into the stability of the protein to pH changes in combination with light, UV absorbance spectra were acquired. The samples incubated at pH 2 and 3 were then irradiated, and the UV signals were detected immediately after the neutralization and upon 4 and 24 h of incubation. The spectra obtained by using freshly prepared samples at pH 7 under light and dark conditions were reported as controls. Light scarcely affected the mAb at both pH 7 and pH 3 (Fig. 4, B and C), even after 24 h-incubation of irradiated samples. For the samples at pH 2 (Fig. S1, A), Ipilimumab exhibited a complex behavior. When the samples were irradiated at pH 2, no relevant differences were appreciable in the UV spectra in comparison to the dark samples (red lines). On the contrary, titrated samples (dark grey lines) showed a spectrum compatible with the presence of aggregates that are known to scatter the light, resulting in a raised baseline at longer wavelengths and an apparent absorption across the entire spectrum. This was more evident in the case of samples treated with light and increasing the time of incubation to 24 h (Fig. S1, A3).

A correlation of the conformational features of Ipilimumab with the grade of exposure of aromatic residues, particularly Tyr residues, was determined by the second derivative of the UV spectra recorded at acidic pH (Fig. 4). The curves for the spectra obtained at pH 2 and 3, after irradiation and neutralization to pH 7, were reported in Fig. 4 A and B, while in C, the curves for the spectra at pH 7 were taken as a reference. The shift of wavelengths in correspondence of the signals at 285, 289, 292 and 295 nm, expected in the second derivative spectrum of the native mAb protein, was monitored. The degree of exposure of tyrosyl residues (α-value) was determined according to Ragone et al. [22]. The α-value is expected to increase and strive to 1 the more the Tyr exposure is closer to the one of an unfolded protein. On the contrary, it decreases the more the residues are hidden in the core of the protein and strives to 0, the more the Tyr exposure is closer to the one of an N-Ac-Tyr-NH_2 and N-Ac-Trp-NH_2 mixture in ethylene glycol (which mimics the environment of the core of a native globular protein). In Fig. 5 D, a bar graph showing the α-value variation is reported. Under acidic conditions, the exposure of tyrosyl residues increased, in accordance with the acid-induced unfolding of the protein. The overall trend of the α-values upon lightening was an increase of the exposure of the tyrosyl residues at all studied pHs. The neutralization of the samples kept in dark at pH 2 and 3 resulted the re-acquisition of the α-values compatible with a native exposure of tyrosyl residues. For the pH 2, this would be in contrast with other results, therefore the decrease of Tyr exposure could be due to aggregation of the protein leading to partially hiding some residues occurring during neutralization. Indeed, a further decrease in the α-values was detected in the samples irradiated and the pH reversed from 2 to 7.

In Table 1 and Table 2, the spectroscopic parameters were summarized. The increase in tyrosyl residue exposure under acidic conditions reflects the acid-induced unfolding of the protein, while light exposure further exacerbated this effect at all pH levels studied. The re-establishment of tyrosyl residue exposure to native levels upon neutralization of pH suggests reversible conformational changes, although the decrease in exposure at pH 2 after neutralization may indicate aggregative processes during the pH reversal.

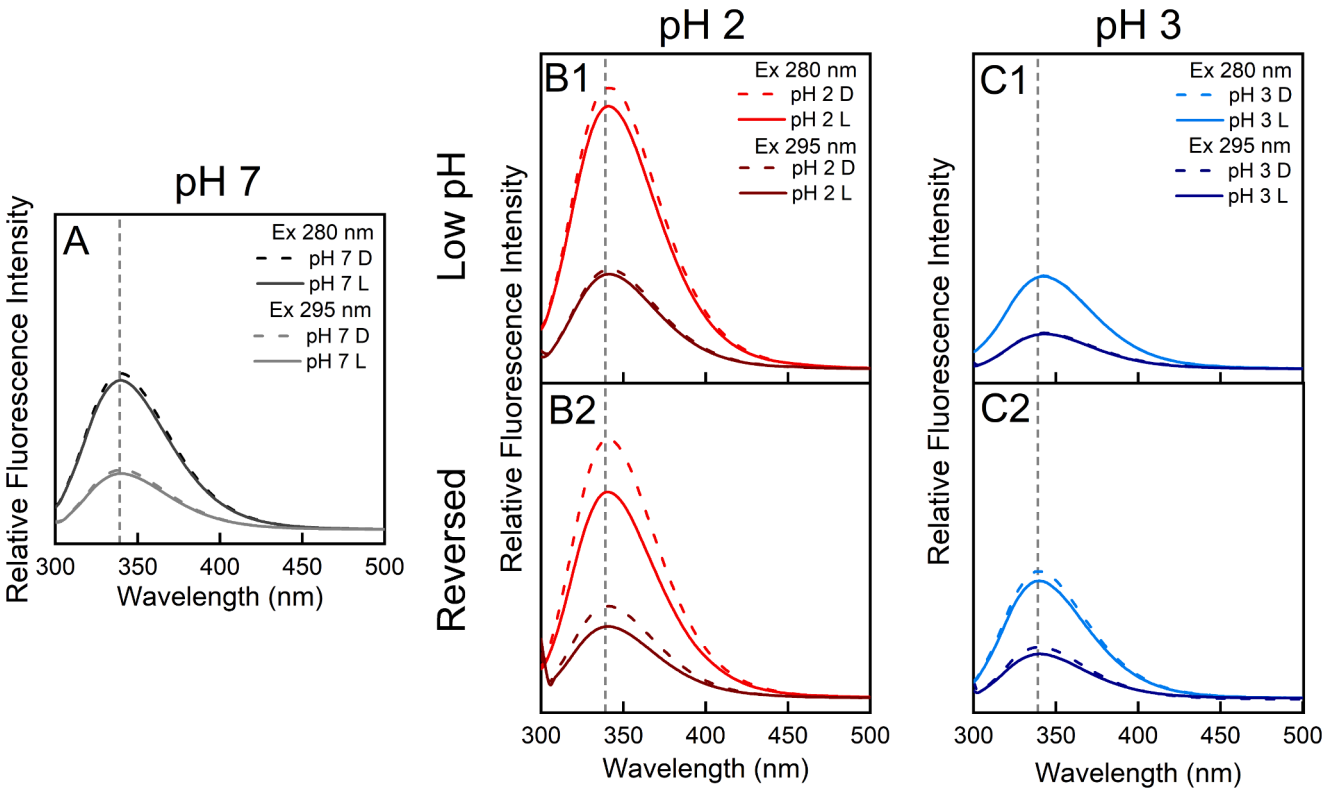

Fig. 3. Fluorescence emission spectra after excitation at 280 and 295 nm of Ipilimumab at pH 7 (A), 2 (B), 3 (C) after exposure to light (L) and followed by neutralization to pH 7 (B2 and C2, respectively for pH 2 and pH 3). The letters L and D indicate light-exposed and dark control samples, respectively. Vertical black dashed lines indicate the wavelength corresponding to the maximum of emission under neutral conditions of pH.

Table 1
Folding parameters of the mAb at various pH and after neutralization from pH 2 and 3 to 7 (REV). The parameters were deduced from far- and near- UV CD, fluorescence measurements and second derivative of the absorbance spectra (α-value). Pf stands for partly folded.

pH								
	2	2 REV	3	3 REV	4	7	9	12
Tertiary structure	no	no	pf	yes	yes	C	yes	no
Secondary structure	no	no	yes	yes	yes	C	yes	no
Wavelength emission shift	red	red	red	no	red	C	blue	blue
α-value	0.88 ± 0.02	0.77 ± 0.01	0.87 ± 0.09	0.72 ± 0.03	0.80 ± 0.04	0.79 ± 0.04	0.70 ± 0.03	0.19 ± 0.04

4. Limited proteolysis of Ipilimumab at pH 2, 3, 7 and upon irradiation

Limited proteolysis has been used to analyze the conformational features of Ipilimumab at low pH (pH 2–3), and its overall sensitivity to proteolysis was compared with that exhibited at pH 7. We used pepsin (EC.3.4.23.1) and proteinase K (EC.3.4.21.64) at acidic and neutral pH, respectively. These proteases display a broad substrate specificity and, therefore, the sites of proteolysis are dictated by the structure and dynamics of the protein substrate, rather than by its amino acid sequence [26,27]. Moreover, pepsin shows the same efficiency of cleavage and the same specificity (preference for certain residues) in the 1–4 pH range [23,28]. Several preliminary experiments were carried out to find out the most suitable enzyme: substrate (E/S) ratio, since very fast and exhaustive proteolysis occurred in Ipilimumab for its relatively poorly compact structure and for the absence of stabilizing excipients, but it is evident that substantial differences in the proteolytic patterns were detectable at pH 3 and pH 2 in the present conditions (Fig. 5).

After 30 min of incubation of protein with pepsin (E/S 1:100) at pH 3 (Fig. 5A), two main species were present into the electrophoretic gel with a molecular weight of ~ 24 and ~ 15 kDa, respectively. The one with lower electrophoretic mobility (Fig. 5A, lane 4–5, 24 kDa) was constituted by two close bands (23 and 24 kDa, respectively) and, upon further incubation for 90 min (Fig. 5B), only one appeared visible into the gel. The other species formed early in the reaction mixture with an apparent MW of ~ 15 kDa was not visible by using a lower E/S ratio, suggesting a reduced proteolysis stability than the higher MW species (not shown). At pH 2, smaller fragments were visible in all the conditions used (Fig. 5A,B), suggesting a very scarce resistance to proteolytic attack, as expected from the fact that the polypeptide chain of Ipilimumab is populating a conformational state characterized by enhanced chain flexibility. Completely different patterns were observed conducting the proteolytic reaction at pH 7 by using proteinase K as a proteolytic enzyme. With a ratio of 1:500 (Fig. 5 A, B, lanes 5–6), no resistant species accumulated in the mixture. However, higher MW species were observed in the sample irradiated at pH 7, likely due to aggregation occurred in the mAb under the effect of light. LC-MS/MS was used for the identification of the proteolytic sites by pepsin at pH 3 analyzing the protein material corresponding to the two main bands (Fig. 5A) by in-gel tryptic digestion. The results were reported in Table S1. The main proteolytic fragments (~23 and ~ 24 kDa) were the light chain (1–215, V_LC_L) and the heavy chain of the Fab (1–225, V_HC_{H1}), respectively. These species after 90-min of incubation were further fragmented by pepsin and their electrophoretic bands were not resolved. Similar pattern was observed with other IgG [29].

Notably, mAb samples, exposed to pH 3 and then neutralized to pH 7, exhibited the same behavior of the samples that did not experience the

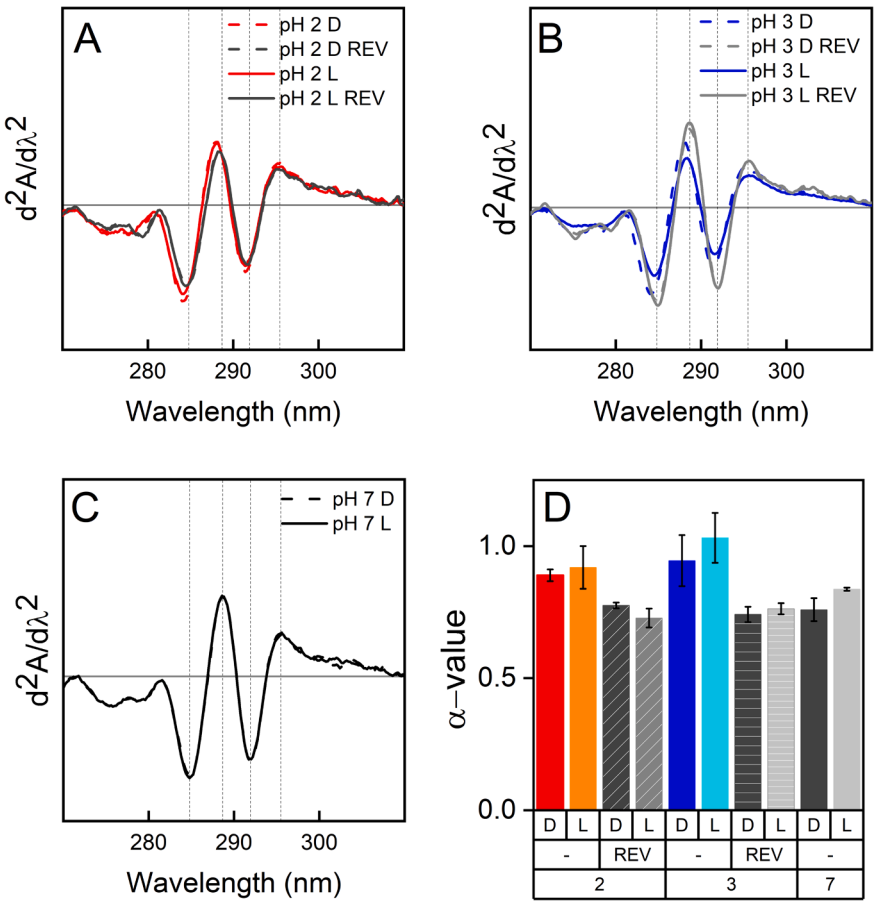

Fig. 4. Second derivative of the absorbance spectra of Ipilimumab at pH 2 (A), 3 (B), 7 (C) after exposure to light (L) and followed by neutralization to pH 7 (REV). The letters L and D indicate light-exposed and dark control samples. The α-values deduced from the second derivative are reported in D.

acidic treatment in contrast to the samples treated at pH 2 (Fig. 5C, REV). This result corroborates the previous spectroscopic data suggesting full conformational reversibility of the protein from pH 3 conditions. When the reaction was repeated reducing the amount of proteinase K (E/S 1:1000), only a few fragments were visible into the gel and the intact Ipilimumab was found in the proteolytic mixture even after 90 min of incubation with the enzyme (Fig. 5D). Light doesn't affect the susceptibility to proteolysis of Ipilimumab (Fig. 5D, lanes indicated with L). Densitometry analysis was conducted, confirming no differences in intensity in the main bands (not shown).

5. Analysis of the physical state of Ipilimumab at low pH and under light by SEC, DLS and electrophoresis

To assess the physical state of Ipilimumab after the simultaneous injury of low pH and light, other analytical assays were performed, such as DLS (Fig. 6), SEC (Fig. 7) and SDS-PAGE (Fig. 8). Ipilimumab was exposed to pH 2 and 3 and then irradiated with 720 kJ/m^2 of artificial light and the samples were analyzed at acidic pH and after neutralization.

DLS profiles of Ipilimumab at pH 7 after light exposure in comparison to the dark samples are reported in Fig. 6A. A main peak was present at a diameter of 11.39 ± 1.22 nm (black line). The data was expressed in "intensity distribution" which gives information about the relative amount of light scattered by the particles in the sample. In the irradiated samples (red line), the presence of aggregates was detected but the monomer diameter didn't change. Similar profiles have been obtained by analyzing samples irradiated at pH 3 (Fig. 6B), with the difference that aggregated molecules were present also in the dark samples. However, the volume distribution profiles displayed a single peak (not shown), suggesting that the extent of aggregation was negligible. The polydispersity index (PDI) was around 0.2 for all the analyzed samples both in the reversed and non-reversed cases, suggesting that the samples were monodisperse and suitable for DLS analysis. The irradiated samples exhibited a slight increase of the PDI to 0.3, indicating a statistically not significant increase in the size distribution of the sample. The size distribution plot of pH 3 treated samples suggested a reacquisition of both native conformation and size after neutralization (Fig. 6B1). At pH 2 (Fig. 6C), Ipilimumab showed the presence of species with higher MW than the monomer (14.02 ± 0.17 nm), but, of note, the overall diameter of these species appeared lower than that of the aggregated ones detected at pH 7 and 3. When the pH was titrated back from 2 to 7 (Fig. 6C1), the distribution profiles shifted to higher MW species in the irradiated and non-irradiated samples, indicating the formation of aggregates, visible also in the volume distribution (Inset, Fig. 6C1). At pH 2, PDI was 0.5 in both irradiated and non-irradiated conditions, implying a significant increase of the size distribution. It increased more when the samples were reversed at pH 7, indeed, PDI was 0.6 (not irradiated) and 0.7 (irradiated), suggesting aggregation and/or precipitation events.

The SEC chromatogram of non-irradiated (protected from light) Ipilimumab samples at pH 7 showed a main peak corresponding to the monomeric species (Fig. 7A, black line). The development of aggregates (Ag), which eluted at 2.4–2.8 mL, was detected in the samples kept at pH 7 and irradiated (Fig. 7A, red line). For the samples exposed to pH 3 and then neutralized to pH 7, an elution volume like the monomeric form at pH 7 was calculated (Fig. 7B, black line). The intensity of the corresponding peak (3.1 mL elution volume) decreased with a concomitant increase of the aggregated species after irradiation (red line) compared to samples kept in dark conditions (black line). The areas of peaks

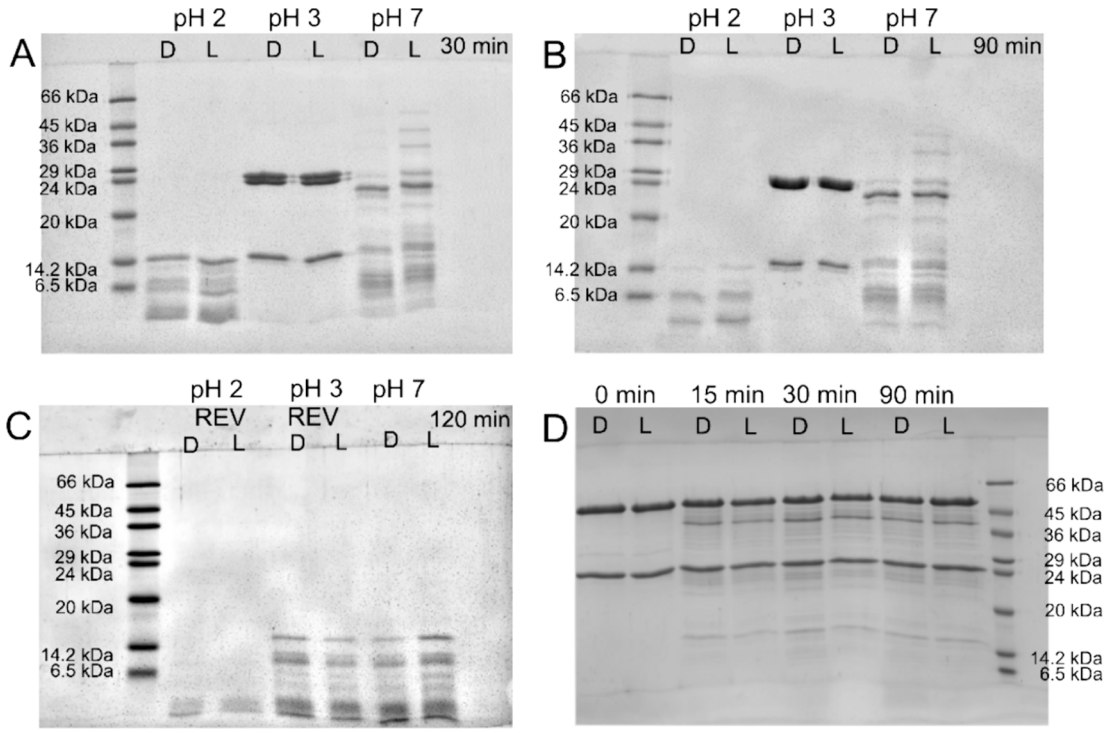

Fig. 5. Limited proteolysis of Ipilimumab by pepsin at acidic pH and proteinase K at neutral pH monitored by SDS-PAGE. The proteolysis mixture after 30 (A) and 90 (B) min of incubation, after titrating back the pH to 7 and 120 min of incubation (C) were reported. The proteolysis reactions were conducted using an enzyme to substrate ratio (E/S) of 1:500 in the case of proteinase K and 1:100 for pepsin. In D, the reaction with proteinase K by using an E/S of 1:1000 is shown. D and L denote the reaction conducted in the dark and after light injury of the sample, respectively.

Table 2
Shift in the maximum emission wavelength (λ) deduced by the fluorescence spectra reported in Fig. 2 for samples exposed to acidic pH and light in comparison to dark samples. The maximum emission wavelength was calculated from the average of three measurements with a standard deviation of 0.1. ΔL-D is the difference between emission λ max in the light and in the dark for each condition, ΔpHD is the difference between emission λ max at acidic pH and pH 7 in the dark and ΔpHL is the difference between emission λ max at acidic pH and pH 7 in the light.

Ex λ (nm)	pH	Em λ max (nm)		ΔL-D	ΔpHD	ΔpHL
		Dark D	Light L			
280	7	339.6	339.9	0.3	0	0.3
295	7	339.6	339.9	0.3	0	0.3
280	2	341.6	341.2	−0.4	2	1.6
280	2 REV	341.1	340.5	−0.6	1.5	0.6
295	2	341.7	341.5	−0.2	2.1	1.6
295	2 REV	340.8	340.8	0.0	1.2	0.9
280	3	342.5	342.5	0.0	2.9	2.6
280	3 REV	339.9	339.9	0.0	0.3	0
295	3	343.3	343.5	0.2	3.7	3.6
295	3 REV	340.3	340.4	0.1	0.7	0.5

(AuTOT) and aggregated species (AuAg) were measured from SEC profiles and expressed as percentage of soluble aggregated species (AuAg/AuTOT × 100). Both at pH 7 and 3, this ratio was roughly 1 %. The intensity of the peak of monomeric Ipilimumab treated at pH 2 and titrated back to pH 7 (Fig. 7C) appeared strongly reduced or even absent. Concomitantly, a peak eluting late just before the signal relative to the total volume was visible (highlighted in the figure). Its elution volume (3.9–4.1 mL) resulted compatible with degraded protein material. Irradiation of the pH 2-samples followed by neutralization to pH 7 (red line) did not seem to induce further effects. Overall, the pH 2 exposed sample underwent degradation and formation of insoluble aggregates. The latter was removed by the filtration operation and were visible in native-PAGE as species not able to enter into the gel (Fig. 7C, inset).

Ipilimumab was analyzed by SDS-PAGE in reducing and non-reducing conditions (Fig. 8). The latter allowed to detect the involvement of disulfide bridges in the eventual degradation process. Ipilimumab showed, in reducing conditions, the two characteristic bands, at ~ 50 kDa for the heavy chain and at ~ 25 kDa for the light chain under all the analyzed pH (Fig. 8A). By irradiating Ipilimumab with 720 kJ/m^2 (lanes denoted with L), only a slight increase of the intensity of the bands at higher MW was detectable. Notably, after neutralization, by using non-reducing conditions, it was possible to detect the presence of aggregates as well as fragments in the samples exposed at pH 2. Specifically, two fragment species produced two intense bands at 46 and 23 kDa, respectively (Fig. 8B). To assess the chemical identity of these species (Fig. 8B), the bands were excised from the gel and a peptide mapping by LC-MS/MS after in gel-digestion was performed. Mass spectrometry analysis indicated the formation of a species containing the $V_HC_{H1}V_LC_L$ domain (46 kDa) with a protein coverage of 90 % and another at lower MW (23 kDa) corresponding to a mixture of V_HC_{H1} and V_LC_L determined by a protein coverage of 100 % (Table S2). The species of 23 kDa could be formed by a cleavage between Ser220 and Cys221 in the HC in analogy with the cleavage occurred by β-elimination between Ser219 and C220 found by Cohen et al. [30]. The possible scheme of fragmentation was reported in Fig. 8C. The formation of these species implied that the light chain could dissociate from the heavy chain by a mechanism that is independent from the reduction of the disulfide bridge holding them together. Similar fragments were formed from a recombinant IgG1 mAb during its long-term storage [30].

The Fig. S1-S3 report also the peptide species containing some chemical modifications present in Ipilimumab after the irradiation. A certain number of oxidations at the level of Trp and Met residues were found, as previously reported. The oxidation involved especially Trp 97 and 149 (V_LC_L), 47, 101 and 108 (V_HC_{H1}). Moreover, the presence of deamidated peptides at the level of Asn and Gln in the irradiated samples was detected in low amounts.

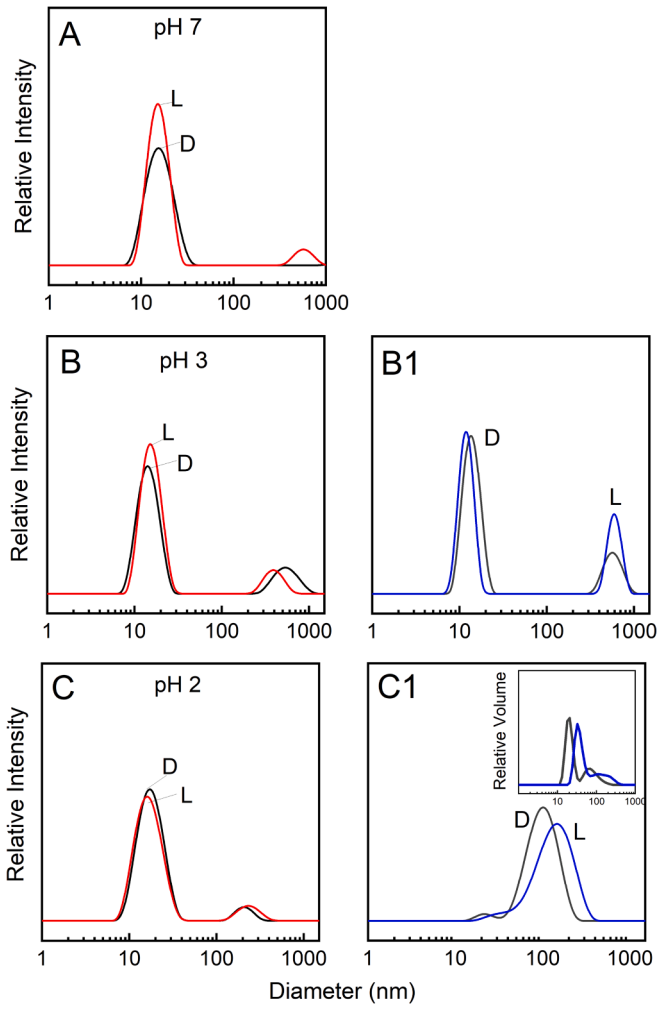

Fig. 6. Physical state of Ipilimumab probed by dynamic light scattering (DLS). The measurements were conducted on protein samples at pH 7 after exposure to light, L (red lines) in comparison with the dark condition, D (black lines) (A), and on mAb samples exposed at acidic pH, irradiated (B, C) and after neutralization (B1, C1). The letters L and D indicate light-exposed and dark control samples. The inset in C1 shows the same measurement expressed in relative volume. Three independent measurements were conducted for each condition. (For interpretation of the references to colour in this figure legend, the reader is referred to the web version of this article.)

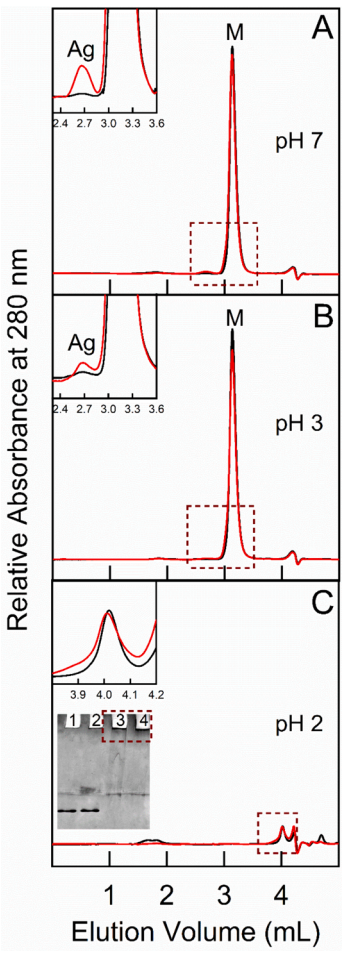

Fig. 7. Physical state of Ipilimumab probed by size exclusion chromatography (SEC). The protein samples at pH 7 (A), 3 (B) and 2 (C), after filtration, were loaded onto a TSKgel® UP-SW3000 column and eluted under the same conditions. The profiles of protected from light samples (black lines) and light exposed samples after neutralization (red lines) were reported. The letter M and Ag close to the peaks indicate monomeric and aggregated species, respectively. Inserts report the zoom of the chromatograms in specific values of elution volume to highlight the aggregate formation in A and B, and the degradation in C. In C, native gel of dark (1, 3) and irradiated (2, 4) samples at pH 3 (1, 2) and pH 2 (3, 4) is reported. (For interpretation of the references to colour in this figure legend, the reader is referred to the web version of this article.)

The samples exposed to pH 2 and irradiated as well as the control samples at pH 7 were also directly analyzed by LC-MS/MS and the LC chromatograms were reported (Fig. 9A,B). In the samples at pH 7 (Fig. 9A), intact mAb eluted at 30 min of retention time, while in the pH 2-exposed samples (Fig. 9B), the intact protein species was not found. In the last samples, a new signal was detectable at RT 25.3 min, absent at pH 7 and 3. Its calculated mass value was 23.4 kDa in accordance with the MW of the light chain (Fig. 9C). Of note, another species was found upon light irradiation containing a Δ mass of −18 Da (Fig. 9D, red star). The reduction of 18 Da could be explained by the loss of a water molecule following the formation of an isopeptide bond between an Asp171 side chain and either one of a Lys, Ser or Thr side chain [31,32].

6. Discussion

The therapeutic potential of mAbs is well known and the market demand for these molecules grows continuously. Nevertheless, the need to optimise the efficiency of their production to improve the yield and reduce the costs is still a critical issue for the pharmaceutical industry [33]. The use of low pH for viral inactivation and for protein A chromatography steps could raise adverse effects on the development of therapeutic antibodies [7,34]. Other contemporary factors may further influence the safe and suitable production of mAbs such as their accidental exposure to environmental light [35]. Moreover, although mAb production follows similar pipelines and the currently used technological platforms are proven and robust, the inherent physicochemical properties of each mAb selectively affect their manufacture and, therefore, should be individually explored. Indeed, a few amino acid differences between homolog proteins can result in their different stability towards different stresses.

The possibility of light exposure during the viral inactivation and protein A chromatography steps is here considered for the therapeutic mAb Ipilimumab. Specifically, we have examined the the effect of pH changes upon simulated sunlight on protein folding. We have found that at pH 2, Ipilimumab undergoes non-reversible unfolding. Fast aggregation with formation of scarcely soluble amorphous aggregates as well as fragmentation were detected when the protein was taken back to neutral conditions. Noteworthy, light exacerbated these two events: aggregation and fragmentation. At pH 3, the unfolding of the protein

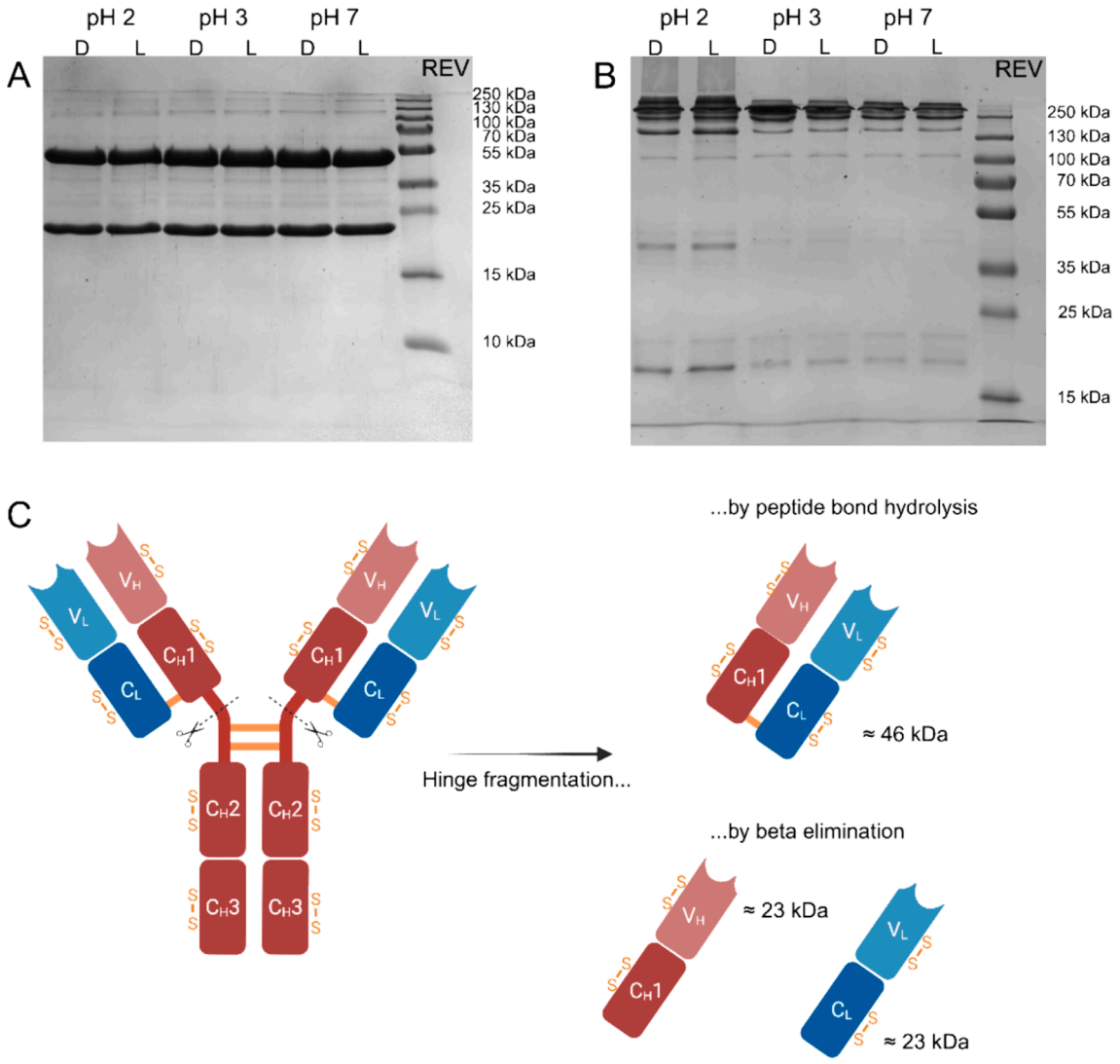

Fig. 8. Physical state of Ipilimumab probed by electrophoresis. The protein samples incubated at different pHs, exposed to light (L) and neutralized to pH 7 (REV) were analyzed by SDS-PAGE in reducing conditions (A) and in non-reducing conditions (B). Scheme of fragmentation of Ipilimumab under acidic conditions (C).

was partial, and the aggregation observed resulted a tolerable and bearable process. Moreover, a remarkable conformational reversibility was detected after neutralization from pH 3 to 7, with the spectroscopic properties of Ipilimumab closely resembling those of the native protein. Therefore, the acid-induced denaturation of Ipilimumab didn't proceed completely at pH values in which it can assume conformations different from the fully unfolded ones. Furthermore, the threshold for Ipilimumab denaturation lies between pH 2 and 3 and is correlated with the loss of the protein structural cooperativity, which is the most critical factor determining whether the protein can refold [36]. In synthesis, it is difficult to predict the exact pH to work with to ensure the protein refolding during the drug scale-up, maximizing the yield of production. However, such pH should allow at least the formation of local structures, which efficiently reduce the conformational space, directing and accelerating the folding process.

Limited proteolysis experiments with pepsin and proteinase K, provided further validation of the spectroscopic findings, elucidating the mAb proteolytic susceptibility under different pH conditions and supporting a strict correlation between folding reversibility and the presence of persistent structured regions in the protein. Even though the sites of proteolysis found at pH 3 and 7 are not immediately comparable, because of the different proteases used, the overall susceptibility to the two protease attacks could be correlated to the inherent conformational property of the substrate. At pH 3, Ipilimumab is populating a partially folded state that is substantially more compact than expected for a random coil state as deduced from our spectroscopic results, and in line with this finding, proteolysis results much more selective than expected for a highly unstructured state. Indeed, proteolysis takes place preferentially at sites located in the loops (hinge region) connecting the two main domains of the mAb, suggesting that some chain regions, folded in the native state, are still enough compact to inhibit the proteolytic attack. By contrast, the loops appear to be largely unstructured and, therefore, susceptible to proteolysis. Conversely, at pH 2, the enhanced proteolytic susceptibility was consistent with the presence of a more flexible conformation, at least in the region encompassing the Fab domain. Thus, it can be concluded that at pH 2, the domains responsible for the structural cooperativity of the mAb are unfolded, and the protein cannot refold into the native conformation. Interestingly, it was reported that the refolding of the isolated Fab (Ranibizumab) appears more effective the faster a near-native intermediate is formed [37]. Moreover, while the CH2 domain of an IgG resulted acid sensitive because the number of ionizable side chains, the stability of the CH1 domain to acid denaturation was considered determinant for the refolding efficiency of the protein [38]. In conclusion, the structural integrity of the Fab or at least the CH1 domain as displayed by Ipilimumab at pH 3 would ensure effective refolding of the protein and a reduced risk of aggregation and

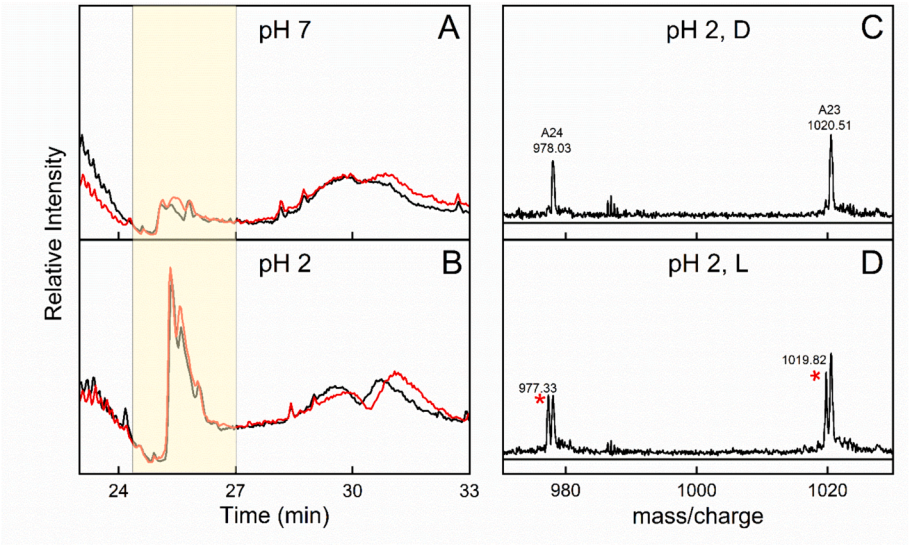

Fig. 9. LC-MS/MS analysis of Ipilimumab samples exposed at pH 2 and neutralized at pH 7 in comparison with the mAb at pH 7. TIC profiles of the samples at pH 7 (A) and pH 2 (B) before (black line) and after (red line) light exposure. Mass to charge spectra corresponding to the region highlighted in yellow in B before (C) and after (D) light exposure. Stars indicate *m/z* signals belonging to the species containing the cyclization (Δ mass −18 Da). (For interpretation of the references to colour in this figure legend, the reader is referred to the web version of this article.)

degradation.

The aggregation constitutes a major concern for the mAb and has been found to be modulated substantially by the drug formulation, buffer composition, and diluents [7,39]. It occurs particularly during the neutralization of the samples from acidic pH. Indeed, at low pH, the presence of a large net positive charge on the protein minimizes both intramolecular and intermolecular interactions thus favoring the solubility of the mAb [12,21]. The electrostatic repulsive forces are abolished by titration to neutrality inducing the observed propensity of the protein for aggregation. This appears particularly critical at pH below 3 for Ipilimumab that populates an extended conformational state where certain regions, and residues, normally hidden in the folded structure become more exposed to solvent and where no folding nuclei are present. Furtherly, in our previous study, we have shown that the light strongly affects the tendency of Ipilimumab to aggregate, especially in dilute solution, as a consequence of modifications of some amino acids and smoothed effects of the excipients commonly preventing aggregation [12]. Here, light-induced aggregation seems to follow a more complex mechanism, depending on the conformational state populated by Ipilimumab. At neutral pH, soluble aggregation appears more extensive than in acidic conditions, where not soluble and irreversible aggregates were formed and little quantity of monomeric species in a dynamic equilibrium with the aggregated ones were found.

Finally, another process emerging during the handling of Ipilimumab under our experimental conditions is the generation of fragments particular evident reversing the pH from 2 to 7. Apparently, temporary exposure to extreme pH values accelerates mAb hinge fragmentation, which has been otherwise reported after prolonged storage at only mildly adverse conditions [40]. The obtained results hint at more than one possible fragmentation mechanism occurring simultaneously, with peptide bond hydrolysis and beta elimination in the hinge region being the most probable culprits for the separation of heavy and light chains as observed in our experiments.

7. Conclusions

Light appears as a minor risk factor for therapeutic mAb manufacturing, since in most cases the production and storage of biopharmaceutics are performed in light-protected conditions. However, light exposure can affect the stability of these proteins and the modifications of their sequence and/or conformation can consequently induce the variation of their physical state, i.e., aggregation and fragmentation [7]. Aggregation is extremely critical for the administration of protein drugs [7,41] and for immunogenic adverse effects on the patient [42].

Under the light doses used in this work, the extent of the chemical modifications was not extensive, but the appearance of a cyclization event is a sign of stressed situation that can lead to important biological and pharmaceutical changes in the active principle. The mechanism of this reaction is beyond the scope of this paper, but it could be speculated that cyclization occurs on a perturbed substrate, in which light represents a key factor that exacerbates the intrinsic protein instability until degradation and permanent damage. As shown in this paper, pH and light stressors can cause aggregation and fragmentation under uncontrolled conditions during mAb production. Light can aggravate the damage induced on the mAbs by low pH conditions. Therefore, we recommend to avoid light exposure during viral sterilization, a process needed during their production for their in-use safety. From our experience, the primary structure and the conformation of a mAb have a great impact on the stability of the molecule under specific stressors [12,41]. We suggest that each therapeutic antibody should be investigated individually to evidence the weak points on their structure to elaborate a set of pH parameters and conditions for their safety and to improve the yield and development of new drugs.

Funding

This project has received funding from the Innovative Medicines Initiative 2 Joint Undertaking (JU) under grant agreement N° 101007939 (RealHOPE). This Joint Undertaking receives support from the European Union's Horizon 2020 research and innovation programme and EFPIA.

CRediT authorship contribution statement

Elena Rizzotto: Writing – review & editing, Methodology, Investigation, Formal analysis, Data curation. **Ilenia Inciardi:** Methodology, Investigation, Formal analysis. **Benedetta Fongaro:** Writing – review & editing, Methodology, Investigation, Formal analysis, Data curation. **Philipp Trolese:** Investigation, Formal analysis. **Giorgia Miolo:** Writing

– review & editing, Visualization, Validation, Supervision, Funding acquisition, Data curation, Conceptualization. **Patrizia Polverino de Laureto:** Writing – review & editing, Writing – original draft, Validation, Supervision, Project administration, Methodology, Investigation, Funding acquisition, Data curation, Conceptualization.

Declaration of competing interest

The authors declare that they have no known competing financial interests or personal relationships that could have appeared to influence the work reported in this paper.

Data availability

Data will be made available on request.

Acknowledgments

The authors thank Eleonora Cecchin and Sarah Prakesch for conducting some measurements, Dr. Marina Coppola and Enrico Gori for providing Ipilimumab.

Author contributions

ER: Visualization, Investigation, Data curation, Formal analysis; II: Formal analysis; BF: Methodology, Software, Validation, Formal analysis; PT: Methodology, Software, Validation, Formal analysis; GM: Conceptualization, Writing- Reviewing, Editing, Resources, Project administration; PPDL: Conceptualization, Writing-Reviewing and Editing, Resources, Project administration, Funding acquisition.

Appendix A. Supplementary data

Supplementary data to this article can be found online at https://doi.org/10.1016/j.ejpb.2024.114387.

Bibliography

[1] F.C. Breedveld, Therapeutic monoclonal antibodies, Lancet 355 (2000) 735–740, https://doi.org/10.1016/S0140-6736(00)01034-5.
[2] M.L. Chiu, D.R. Goulet, A. Teplyakov, G.L. Gilliland, Antibody structure and function: The basis for engineering therapeutics, Antibodies (basel) 8 (2019) 55–135, https://doi.org/10.3390/antib8040055.
[3] D.R. Davies, H. Metzger, Structural basis of antibody function, Annu. Rev. Immunol. 1 (1983) 87–115, https://doi.org/10.1146/annurev.iy.01.040183.000511.
[4] M. Vázquez-Rey, D.A. Lang, Aggregates in monoclonal antibody manufacturing processes, Biotechnol. Bioeng. 108 (2011) 1494–1508, https://doi.org/10.1002/bit.23155.
[5] R.L. Fahrner, H.L. Knudsen, C.D. Basey, W. Galan, D. Feuerhelm, M. Vanderlaan, G. S. Blank, Industrial purification of pharmaceutical antibodies: Development, operation, and validation of chromatography processes, Biotechnol. Genet. Eng. Rev. 18 (2001) 301–327, https://doi.org/10.1080/02648725.2001.10648017.
[6] A.R. Mazzer, X. Perraud, J. Halley, J. O'Hara, D.G. Bracewell, Protein A chromatography increases monoclonal antibody aggregation rate during subsequent low pH virus inactivation hold, J. Chromatogr. A 1415 (2015) 83–90, https://doi.org/10.1016/j.chroma.2015.08.068.
[7] N.A. Kim, S. Kar, Z. Li, T.K. Das, J.F. Carpenter, Mimicking low pH virus inactivation used in antibody manufacturing processes: Effect of processing conditions and biophysical properties on antibody aggregation and particle formation, JPharmSci 110 (2021) 3188–3199, https://doi.org/10.1016/j.xphs.2021.06.002.
[8] A.A. Shukla, B. Hubbard, T. Tressel, S. Guhan, D. Low, Downstream processing of monoclonal antibodies—Application of platform approaches, J. Chromatogr. B 848 (2007) 28–39, https://doi.org/10.1016/j.jchromb.2006.09.026.
[9] T.E. Creighton, N.J. Darby, J. Kemmink, The roles of partly folded intermediates in protein folding, FASEB J. 10 (1996) 110–118, https://doi.org/10.1096/fasebj.10.1.8566531.
[10] S. Gupta, W. Jiskoot, C. Schöneich, A.S. Rathore, Oxidation and deamidation of monoclonal antibody products: Potential impact on stability, biological activity, and efficacy, J. Pharm. Sci. 111 (2022) 903–918, https://doi.org/10.1016/j.xphs.2021.11.024.
[11] J. Nieva, P. Wentworth, The antibody-catalyzed water oxidation pathway – a new chemical arm to immune defense? Trends Biochem. Sci 29 (2004) 274–278, https://doi.org/10.1016/j.tibs.2004.03.009.
[12] B. Fongaro, V. Cian, F. Gabaldo, G. De Paoli, G. Miolo, P. Polverino de Laureto, Managing antibody stability: Effects of stressors on Ipilimumab from the commercial formulation to diluted solutions, Eur J Pharm Biopharm 176 (2022) 54–74, https://doi.org/10.1016/j.ejpb.2022.05.005.
[13] G. Vidarsson, G. Dekkers, T. Rispens, IgG subclasses and allotypes: From structure to effector functions, Front. Immunol. 5 (2014) 1–17.
[14] T. Ito, K. Tsumoto, Effects of subclass change on the structural stability of chimeric, humanized, and human antibodies under thermal stress, Protein Sci. 22 (2013) 1542–1551, https://doi.org/10.1002/pro.2340.
[15] P. Arosio, S. Rima, M. Morbidelli, Aggregation mechanism of an IgG2 and two IgG1 monoclonal antibodies at low pH: From oligomers to larger aggregates, Pharm Res 30 (2013) 641–654, https://doi.org/10.1007/s11095-012-0885-3.
[16] A. Goyon, M. Excoffier, M.-C. Janin-Bussat, B. Bobaly, S. Fekete, D. Guillarme, A. Beck, Determination of isoelectric points and relative charge variants of 23 therapeutic monoclonal antibodies, J. Chromatogr. B 1065–1066 (2017) 119–128, https://doi.org/10.1016/j.jchromb.2017.09.033.
[17] J.F. Grosso, M.N. Jure-Kunkel, CTLA-4 blockade in tumor models: an overview of preclinical and translational research, Cancer Immun 13 (2013) 5, https://doi.org/10.1158/1424-9634.DCL-5.13.1.
[18] U.A. Ramagopal, W. Liu, S.C. Garrett-Thomson, J.B. Bonanno, Q. Yan, M. Srinivasan, S.C. Wong, A. Bell, S. Mankikar, V.S. Rangan, S. Deshpande, A. J. Korman, S.C. Almo, Structural basis for cancer immunotherapy by the first-in-class checkpoint inhibitor ipilimumab, Proc. Natl. Acad. Sci. 114 (2017) E4223–E4232, https://doi.org/10.1073/pnas.1617941114.
[19] A. Sreedhara, J. Yin, M. Joyce, K. Lau, A.T. Wecksler, G. Deperalta, L. Yi, Y. John Wang, B. Kabakoff, R.S.K. Kishore, Effect of ambient light on IgG1 monoclonal antibodies during drug product processing and development, Eur J Pharm Biopharm 100 (2016) 38–46, https://doi.org/10.1016/j.ejpb.2015.12.003.
[20] S.B. Hari, H. Lau, V.I. Razinkov, S. Chen, R.F. Latypov, Acid-induced aggregation of human monoclonal IgG1 and IgG2: Molecular mechanism and the effect of solution composition, Biochemistry 49 (2010) 9328–9338, https://doi.org/10.1021/bi100841u.
[21] R. Wälchli, M. Ressurreição, S. Vogg, F. Feidl, J. Angelo, X. Xu, S. Ghose, Z. Jian Li, X. Le Saoût, J. Souquet, H. Broly, M. Morbidelli, Understanding mAb aggregation during low pH viral inactivation and subsequent neutralization, Biotechnol. Bioeng. 117 (2020) 687–700, https://doi.org/10.1002/bit.27237.
[22] R. Ragone, G. Colonna, C. Balestrieri, L. Servillo, G. Irace, Determination of tyrosine exposure in proteins by second-derivative spectroscopy, Biochemistry 23 (1984) 1871–1875, https://doi.org/10.1021/bi00303a044.
[23] J.S. Fruton, The Specificity and Mechanism of Pepsin Action, in: Advances in Enzymology and Related Areas of Molecular Biology, John Wiley & Sons Ltd, 1970, pp. 401–443, https://doi.org/10.1002/9780470122785.ch9.
[24] W. Ebeling, N. Hennrich, M. Klockow, H. Metz, H.D. Orth, H. Lang, Proteinase K from tritirachium album limber, Eur. J. Biochem. 47 (1974) 91–97, https://doi.org/10.1111/j.1432-1033.1974.tb03671.x.
[25] U.K. Laemmli, Cleavage of structural proteins during the assembly of the head of bacteriophage T4, Nature 227 (1970) 680–685, https://doi.org/10.1038/227680a0.
[26] P. Polverino de Laureto, E. Frare, R. Gottardo, H. van Dael, A. Fontana, Partly folded states of members of the lysozyme/lactalbumin superfamily: A comparative study by circular dichroism spectroscopy and limited proteolysis, Protein Sci. 11 (2002) 2932–2946, https://doi.org/10.1110/ps.0205802.
[27] A. Fontana, P. Polverino de Laureto, V. de Filippis, E. Scaramella, M. Zambonin, Limited proteolysis in the study of protein conformation, in: E.E. Sterchi, W. Stöcker (Eds.), Proteolytic Enzymes, Tools and Targets, Springer, Berlin, Heidelberg, 1999, pp. 253–280, 10.1007/978-3-642-59816-6_15.
[28] B.M. Dunn, M. Jimenez, B.F. Parten, M.J. Valler, C.E. Rolph, J. Kay, A systematic series of synthetic chromophoric substrates for aspartic proteinases, Biochem. J 237 (1986) 899–906, https://doi.org/10.1042/bj2370899.
[29] K. Inouye, S. Ohnaka, Pepsin digestion of a mouse monoclonal antibody of IgG1 class formed F(ab')2 fragments in which the light chains as well as the heavy chains were truncated, J. Biochem. Bioph. Methods 48 (2001) 23–32, https://doi.org/10.1016/S0165-022X(00)00141-X.
[30] S.L. Cohen, C. Price, J. Vlasak, β-elimination and peptide bond hydrolysis: Two distinct mechanisms of human IgG1 hinge fragmentation upon storage, J. Am. Chem. Soc. 129 (2007) 6976–6977, https://doi.org/10.1021/ja0705994.
[31] L. Grassi, C. Cabrele, Susceptibility of protein therapeutics to spontaneous chemical modifications by oxidation, cyclization, and elimination reactions, Amino Acids 51 (2019) 1409–1431, https://doi.org/10.1007/s00726-019-02787-2.
[32] H.C. Hayes, L.Y.P. Luk, Y.-H. Tsai, Approaches for peptide and protein cyclisation, Org. Biomol. Chem. 19 (2021) 3983–4001, https://doi.org/10.1039/D1OB00411E.
[33] A.L. Grilo, A. Mantalaris, The increasingly human and profitable monoclonal antibody market, Trends Biotechnol 37 (2019) 9–16, https://doi.org/10.1016/j.tibtech.2018.05.014.
[34] D. Ejima, K. Tsumoto, H. Fukada, R. Yumioka, K. Nagase, T. Arakawa, J.S. Philo, Effects of acid exposure on the conformation, stability, and aggregation of monoclonal antibodies, Proteins: Structure, Function, and Bioinformatics 66 (2007) 954–962, https://doi.org/10.1002/prot.21243.
[35] D.I. Pattison, A.S. Rahmanto, M.J. Davies, Photo-oxidation of proteins, Photochem. Photobiol. Sci. 11 (2011) 38–53, https://doi.org/10.1039/C1PP05164D.
[36] R. Seckler, R. Jaenicke, Protein folding and protein refolding, FASEB J 6 (1992) 2545–2552, https://doi.org/10.1096/fasebj.6.8.1592207.

[37] K. Gani, R. Bhambure, P. Deulgaonkar, D. Mehta, M. Kamble, Understanding unfolding and refolding of the antibody fragment (Fab). I. *In-vitro* study, Biochem. Eng. J. 164 (2020) 107764, https://doi.org/10.1016/j.bej.2020.107764.
[38] M. Hebditch, R. Kean, J. Warwicker, Modelling of pH-dependence to develop a strategy for stabilising mAbs at acidic steps in production, Comput. Struct. Biotechnol. J. 18 (2020) 897–905, https://doi.org/10.1016/j.csbj.2020.03.002.
[39] B.D. Mason, L. Zhang, R.L. Remmele, J. Zhang, Opalescence of an IgG2 monoclonal antibody solution as it relates to liquid–liquid phase separation, JPharmSci 100 (2011) 4587–4596, https://doi.org/10.1002/jps.22650.
[40] J. Vlasak, R. Ionescu, Fragmentation of monoclonal antibodies, Mabs 3 (2011) 253–263, https://doi.org/10.4161/mabs.3.3.15608.
[41] E. De Diana, E. Rizzotto, I. Inciardi, L. Menilli, M. Coppola, P. Polverino de Laureto, G. Miolo, Towards a better understanding of light-glucose induced modifications on the structure and biological activity of formulated Nivolumab, Int. J. Pharm. 654 (2024) 123926, https://doi.org/10.1016/j.ijpharm.2024.123926.
[42] M. Nabhan, M. Pallardy, I. Turbica, Immunogenicity of bioproducts: cellular models to evaluate the impact of therapeutic antibody aggregates, Front Immunol 11 (2020) 725–733, https://doi.org/10.3389/fimmu.2020.00725.